

DISCOVERY OF AHRENSITE $\gamma\text{-Fe}_2\text{SiO}_4$ AND TISSINTITE $(\text{Ca},\text{Na},\square)\text{AlSi}_2\text{O}_6$: TWO NEW HIGH PRESSURE MINERALS FROM THE TISSINT MARTIAN METEORITE. Chi Ma¹, Oliver Tschauner², Yang Liu³, John R. Beckett¹, George R. Rossman¹, Kirill Zuravlev⁴, Vitali Prakapenka⁴, Przemyslaw Dera⁴, Stanislav Sinogeikin⁵, Jesse Smith⁵, Lawrence A. Taylor⁶; ¹California Institute of Technology, Pasadena, CA 91125, USA; ²University of Nevada, Las Vegas, NV 89154, USA; ³Jet Propulsion Laboratory, California Institute of Technology, Pasadena, CA 91109, USA; ⁴CARS, University of Chicago, Argonne National Laboratory, Argonne, IL 60439, USA; ⁵HPCAT, Argonne National Laboratory, Argonne, IL 60439, USA; ⁶Planetary Geosciences Institute, University of Tennessee, Knoxville, TN 37996, USA; Email: chi@gps.caltech.edu.

Introduction: The recent Martian meteorite fall, Tissint, is a fresh heavily shocked olivine-phyric shergottite [1]. During a nanomineralogy investigation of this meteorite by analytical scanning electron microscope, electron probe, micro-Raman, and synchrotron diffraction, we identified two new shock-induced minerals ahrensite, $\gamma\text{-Fe}_2\text{SiO}_4$, and tissintite, $(\text{Ca},\text{Na},\square)\text{AlSi}_2\text{O}_6$; these phases provide new insights into shock conditions and impact processes on Mars. Both were approved by the Commission on New Minerals, Nomenclature and Classification of the International Mineralogical Association. In this work, we describe these new minerals and demonstrate how nanomineralogy can play a unique role in meteorite and Mars rock research.

Ahrensite (IMA 2013-028): Ahrensite ($\gamma\text{-Fe}_2\text{SiO}_4$) is the polymorph of fayalite with a cubic spinel structure and the Fe-analog of ringwoodite ($\gamma\text{-Mg}_2\text{SiO}_4$). Synthetic $\gamma\text{-Fe}_2\text{SiO}_4$ is a well known high-pressure (P) form of fayalite [2]. Natural occurrences are also known [3,4,5] but our study provides the first full chemical and structural characterization that establishes ahrensite, $\gamma\text{-Fe}_2\text{SiO}_4$, as a new mineral. The name honors Thomas J. Ahrens (1936-2010), a geophysicist at the California Institute of Technology, for his many fundamental contributions to high-pressure mineral physics research.

Both ahrensite and ringwoodite are found in Tissint as fine-grained polycrystalline aggregates in the rims of olivines adjacent to shock-melt pockets (Figs. 1-2) but they preserve the Mg-Fe gradient of the original olivine crystal. They are often separated from the melt pocket by a thin layer of amorphous $(\text{Mg},\text{Fe})\text{SiO}_3$ and wüstite $(\text{Fe},\text{Mg})\text{O}$. Ahrensite occurs as translucent, bluish-green, 5–20 μm polycrystalline aggregates consisting of submicron-sized crystals of 50–400 nm in diameter with grain size generally increasing towards the melt pocket (Fig. 3). The mean chemical composition of the type region is (wt%) SiO₂ 34.95, FeO 43.76, MgO 21.15, MnO 0.75, sum 100.61 with an empirical formula of $(\text{Fe}_{1.06}\text{Mg}_{0.91}\text{Mn}_{0.02})\text{Si}_{1.01}\text{O}_4$. Synchrotron micro-diffraction reveals that ahrensite has a cubic spinel structure with space group $Fd\bar{3}m$. A synchrotron diffraction refinement suggests that some of the Fe is on site 8a, leading to a formula of

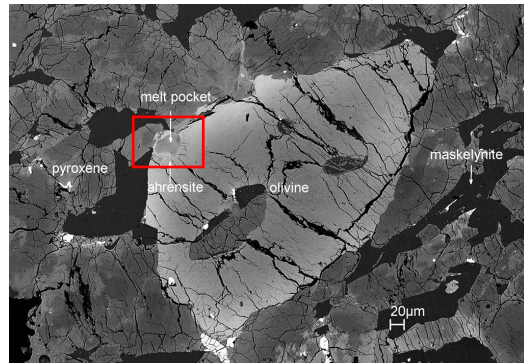


Fig. 1. Back-scatter electron (BSE) image showing ahrensite and shock melt pocket in Tissint section UT2. Red box marks location of Fig. 2.

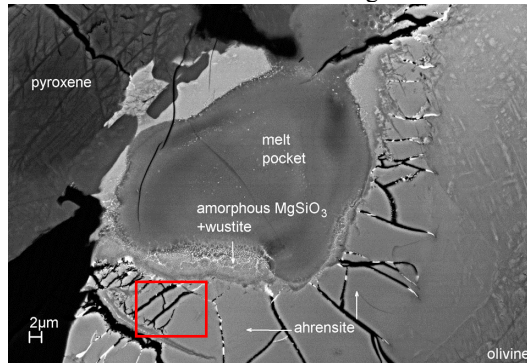


Fig. 2. Enlarged BSE image of Fig. 1, revealing ahrensite domains with surrounding phases. Red box marks location of Fig. 3.

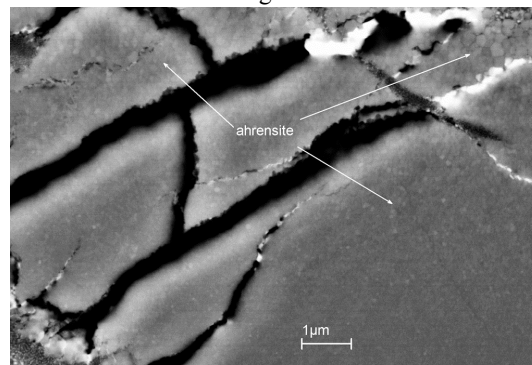


Fig. 3. BSE image of a portion of Fig. 2, revealing submicrometer- to nanometer-sized polycrystalline ahrensite.

$(\text{Fe}_{1.12}\text{Mg}_{0.86}\text{Si}_{0.02})(\text{Si}_{0.98}\text{Fe}_{0.02})\text{O}_4$, although the excess Fe is within error of zero. The cell parameters are $a =$

$8.163(1) \text{ \AA}$, $V = 543.96(7) \text{ \AA}^3$, $Z = 8$, which leads to a calculated density of 4.135 g/cm^3 .

Tissintite (IMA 2013-027): Tissintite, $(\text{Ca},\text{Na},\square)\text{AlSi}_2\text{O}_6$, is the Ca-analog of jadeite with $\frac{1}{4}$ of the $M2$ Ca/Na sites vacant and a likely end-member of $(\text{Ca}_{0.75}\square_{0.25})\text{Al}(\text{Si}_{1.5}\text{Al}_{0.5})\text{O}_6$. The phase exhibits considerable solid solution towards the Ca-Eskola pyroxene (Px) component (CaEs: $(\text{Ca}_{0.5}\square_{0.5})\text{AlSi}_2\text{O}_6$). Based on Px nomenclature [6], tissintite may be considered the Al-analog of omphacite with Al dominant in the $M1$ site and the Si analog of kushiroite with Si dominant in the T site. Synthetic $(\text{Ca},\text{Na},\square)\text{AlSi}_2\text{O}_6$ is not known. Reported here is its first natural occurrence. The mineral name is after the locality, Tissint, Morocco, where the Tissint meteorite fell.

Tissintite occurs as fine-grained aggregates of $0.5\text{--}3 \mu\text{m}$ single crystals in plagioclase (Plag) glass, surrounded by diopside and fayalite within shock-melt pockets (Figs. 4–6). The mean chemical composition of is (wt%) SiO_2 52.52, Al_2O_3 29.61, CaO 13.14, Na_2O 3.89, FeO 0.93, MgO 0.18, sum 100.27, with an empirical formula of $(\text{Ca}_{0.48}\text{Na}_{0.26}\square_{0.26})(\text{Al}_{0.98}\text{Fe}_{0.03}\text{Mg}_{0.01})(\text{Si}_{1.79}\text{Al}_{0.21})\text{O}_6$. Synchrotron and electron back-scatter diffraction reveal that tissintite has the $C2/c$ clinopyroxene structure. The cell parameters are $a = 9.418 \text{ \AA}$, $b = 8.562 \text{ \AA}$, $c = 5.219 \text{ \AA}$, $\beta = 107.56^\circ$, $V = 401.23 \text{ \AA}^3$, $Z = 4$, which leads to a calculated density of 3.395 g/cm^3 .

Origin and significance: Both ahrensite and tissintite are high-P minerals formed by shock metamorphism during the impact event(s) on Mars that led to the excavation and ejection of Tissint off the planet.

Ahrensite and ringwoodite in Tissint are high-P phases apparently formed by solid-state transformation of olivine without significant diffusion, given preservation of Mg-Fe zoning from the original olivine. Crystal size increases towards the melt pocket (Fig. 3), reflecting higher temperatures (T) as the interface is approached. With increasing shock T, olivine transformed to ahrensite (or ringwoodite), then to wüstite ($\text{Fe,Mg}\text{O}$) [or periclase ($\text{Mg,Fe}\text{O}$)] and metasilicate ($\text{Mg,Fe}\text{SiO}_3$) glass at the contact with melt pockets.

Synthetic tissintite is unknown and it has not been reported in any other meteorite or in a terrestrial rock. Constraints on origin must therefore be derived from composition and petrography. Plag or maskelynite (Msk) with a composition between $\text{Ab}_{66.7}\text{An}_{33.3}$ and An_{100} is consistent with a tissintite-type Px whose composition lies on the join between $(\text{Na}_{0.50}\text{Ca}_{0.25}\square_{0.25})\text{AlSi}_2\text{O}_6$ and end-member tissintite, $(\text{Ca}_{0.75}\square_{0.25})\text{Al}(\text{Si}_{1.5}\text{Al}_{0.5})\text{O}_6$. Type tissintite is close to the midpoint of this join $(\text{Ca}_{0.50}\text{Na}_{0.25}\square_{0.25})\text{Al}(\text{Si}_{1.75}\text{Al}_{0.25})\text{O}_6$; its nearly 50% CaEs is the highest known in either a synthetic or natural material. Given its composition and location in the

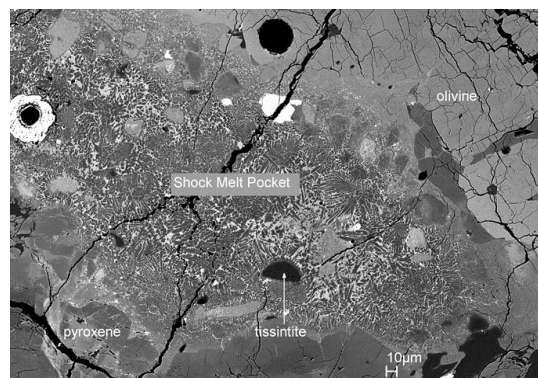


Fig. 4. BSE image showing tissintite in a shock melt pocket in Tissint section UT2.

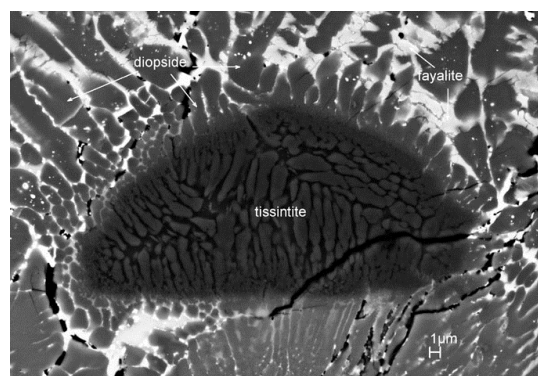


Fig. 5. Enlarged BSE image of Fig. 4 of fine-grained tissintite with surrounding diopside and fayalite.

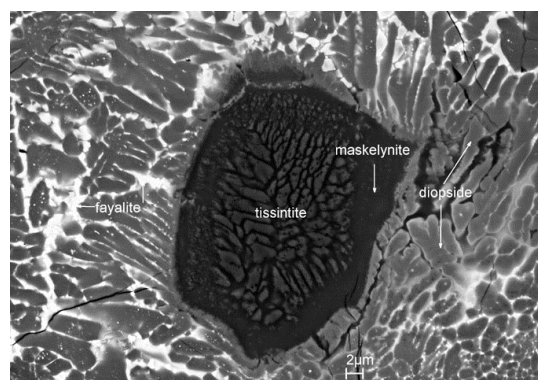


Fig. 6. BSE image showing tissintite crystals within Msk with surrounding diopside and fayalite in a melt pocket in Tissint section UT1.

midst of melt pockets, tissintite probably formed at high P-T, perhaps via Msk melt or solid-state transformation of Msk, with higher T or cooling rates slower than for Msk outside melt pockets key to its formation.

References: [1] Baziotis I. et al. (2013) *Nature Comm.* 4:1404. [2] Ringwood A. (1958) *GCA* 15:18. [3] Xie Z. et al. 2002. *Am. Mineral.* 87:1257. [4] Díaz-Martínez E. & Ormö J. 2003. *LPSC* 34:A1318. [5] Feng L. et al. 2011. *Am. Mineral.* 96:1480. [6] Morimoto N. et al. 1988. *Am. Mineral.* 73:1123.